Proceedings of the IASS 2024 Symposium
Redefining the Art of Structural Design
August 26-30, 2024, Zurich Switzerland
Philippe Block, Giulia Boller, Catherine DeWolf,
Jacqueline Pauli, Walter Kaufmann (eds.)

Maximizing Number of States of Self-Stress in Spanning Grid-Shells

Arek MAZUREK*, William F BAKER[a]

*HKS Inc
125 S Clark St. #1100, Chicago, IL 60603, USA
amazurek@hksinc.com

[a] Skidmore, Owings and Merrill, LLP

Abstract

Efficiency of spanning grid-shells is highly dependent on their 3D form. It is well known that high efficiency of grid like structures is obtained by making them funicular – by forming them in a way they resist the imposed loads mostly axially rather than through bending of their individual members. One of the methods to increase the number of different loads for which a spanning grid-shell remains funicular is to increase the number of independent states of self-stress of its horizontal projection. The number of states of self-stress of a projection depends not only on the number of nodes and bars but also on the location of the nodes. The paper discusses an efficient method to maximize the number of states of self-stress in grid-shells by placing their nodes in locations informed by an Airy stress function. Plane-faced Airy stress functions can be seen as spanning surfaces above the horizontal projections of grid-shells. The proposed method leads to a family of solutions rather than one and also allows finding only a part of available stresses if desired by the designer.

Keywords: States of Self-Stress, Grid-Shells, Airy Stress Function, Force Density, Form Finding, Optimization

1. Introduction

Grid-shells are discrete structural systems where interconnected beams (bars or struts) create shell-like forms. Often, spaces between the beam elements are glazed to create spectacular glazed roofs covering atria or vestibules. The efficiency of these systems is dependent on load paths starting from the surface of the glass, through grid elements to the points of support. It is observed that structural efficiency of these systems is increased when primary load paths are through axial loading of their members. Therefore, forming the shape of a grid-shell in a way that most dominant load combinations result in minimal or no bending moments is a very important initial step of design of a structurally efficient grid-shell.

Grid-shell shown in Figure 1 covers a courtyard of British Museum building in London, UK. The roof has been constructed on top of existing buildings around the perimeter of the courtyard. Its shape is formed to eliminate horizontal thrust on these existing buildings. Because the grid-shell is fully triangulated, number of states of self-stress of its horizontal projection equals to the number of internal nodes (Maxwell [1])

Figure 2 shows an unbuild design for a spanning grid-shell. The grid-shell contains mostly quad panels to reduce complexities of connections and to minimize number of sharp grazed corners common in triangular frames. Lack of triangular panels greatly reduces the number of states of self-stress. The maximum number of the independent stress in the projection of this grid-shell equals to number of intermediate arches on each side $(6 \times 2 + 2 \times 1 = 14)$ plus number of possible stresses of the center portion of the roof which is at least one.

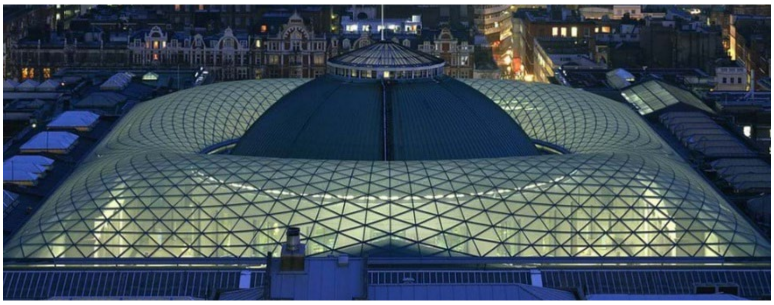

Figure 1: British Museum Roof, London, UK

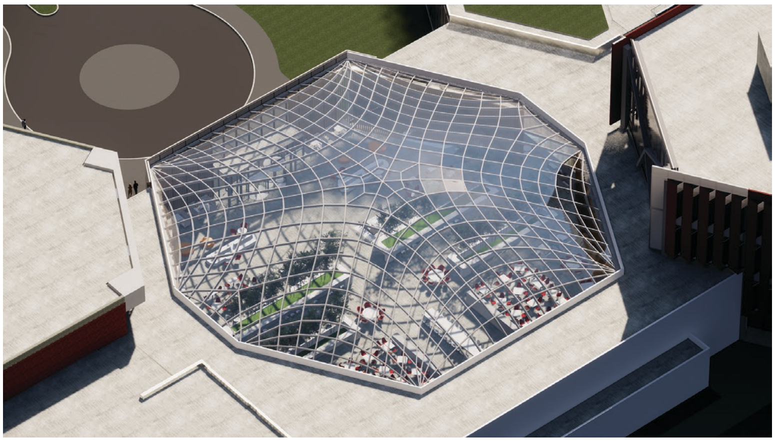

Figure 2: Grid-shell with predominately quad panels.

2. What are the states of self-stress and mechanisms?

The *state of self-stress* of a structure is considered here as a non-zero state of stress of 3D structure where its horizontal 2D projection is in static equilibrium with no external loads. The structures investigated in this paper are axial only systems. These structures can have multiple linearly independent states of self-stress.

A *mechanism* is considered here as an infinitesimal motion that can occur in the horizontal projection of a structure without changing the length of any bar and thus has no effect on its state of stress. The structures can have multiple linearly independent mechanisms.

In general, structures can have multiple states of self-stress and multiple linearly independent mechanisms concurrently.

3. Force density

Force density is defined as the value of an axial load in a truss member divided by its length. The force density for 3D truss members will be equal to the force density of their projections. This is because in a projection the force and the length are reduced by the same factor.

Force density form finding method has been developed by Scheck [2] to find forms of 3D tensile structures. Having force density values as constant leads to a set of linear equations. The solution of these equations results in a truss structure that is in 3D equilibrium.

4. Airy stress function

Airy stress function φ represents 2D state of stress with the following equations:

$$\sigma_{xx} = \varphi_{,yy} = \frac{\partial^2 \varphi}{\partial y^2};\ \sigma_{yy} = \varphi_{,xx} = \frac{\partial^2 \varphi}{\partial x^2};\ \sigma_{xy} = -\varphi_{,xy} = -\frac{\partial^2 \varphi}{\partial x \partial y} \tag{1}$$

An airy stress function for a 2D structure or a 2D projection of a structure is a 3D surface "spanning" above in the 3rd dimension. The unit of the Airy stress function is length-force. A slope of an Airy surface is in units of force. Stress in the structure represented by an Airy stress function equals to a double differentiation of Airy stress surface in the direction perpendicular to the measured stress. Therefore, the stress value in the structure equals the change of slope (curvature) of the Airy stress function. For special cases we can say:

a) Airy stress function spanning above a region of structure without stress is planar.
b) Airy stress function shows smooth curvature above areas with distributed stress and sharp change of slope in areas of concentrated load/force (i.e., discrete trusses).

Examples of Airy stress function for simple balanced forces are shown in Figure 3 where the resultant force is a difference in slopes of Airy stress function on both sides of the integrated width.

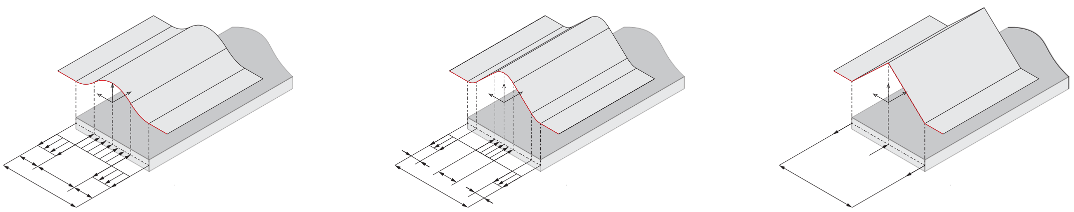

Figure 3: Integrating Airy stress function to obtain resultant forces.

The same can also be concluded with the equation (2), where total stress, within a distance a from a point, equals to the change of slopes of Airy stress function over the $2a$ distance. Interesting to note here is that the resultant of stress does not depend on the shape of the Airy stress function within the distance a. Also, resultant load between points with the same slope of Airy stress function equals zero.

$$\int_{-a}^{a} \sigma_{xx} dy = \int_{-a}^{a} \frac{\partial^2 \varphi}{\partial y^2} dy = \left.\frac{\partial \varphi}{\partial y}\right|_{-a}^{a} \quad (2)$$

5. Why are states of self-stress important in spanning grid shells?

As noted above the best structurally performing grid-shells are generally found to transfer dominant, typically self-weight gravity, loads via axial compression or tension of its members. Imposing flexural loads on longitudinal members is typically considered inefficient. Self-weight gravity loads are not the only ones that govern the design of grid-shells. These structures need to resist uneven patterns of live or snow loads, lateral wind or seismic loads and need to address unintentional support movements, temperature loads and local and global stability concerns. Grid-shells that exhibit only a single state of self-stress of their vertical projection can be funicular (no bending of its members) to only a single load distribution. All other loads will partially or entirely depend on flexural stiffness and flexural strength of the members. Maximizing the number of states of self-stress in grid-shells reduces dependency on the inefficient flexural performance of the structural members.

Consider a simple structure from Figure 4. Funicular loads generate no bending moments where a planar framing transfers the load via bending only. Loads in grid-shell that are not funicular generate partial axial forces and moment.

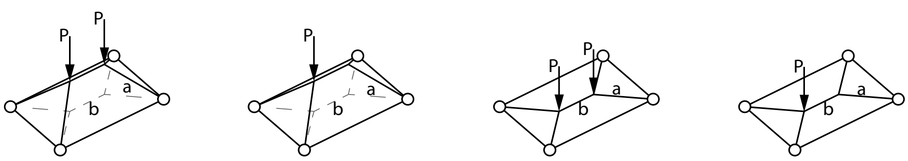

M_{max} =0, $M_{max} = Pb/6$, $M_{max} = Pb$, $M_{max} = 2Pb/3$,

$\boldsymbol{M_{design} = Pb/6}$, $a = b/\cos(45°)$, $\boldsymbol{M_{design} = Pb}$

Figure 4: Funicular and non-funicular loads and the corresponding design moments

Even so the structure is not funicular to this load the bending moments are reduced as compared to the bending only option. Structures funicular to larger number of loads will tend to have less flexure and potentially be more efficient.

6. Pseudo algorithm in finding proper count

For any 2D planar projection of a 3D truss structure that is in equilibrium, a plane-faced Airy stress function can be constructed. The Airy stress function spans above the 2D projection of the structure. The change of slopes across adjacent planar faces equal to the values of members forces projected on the 2D plane. Number of linearly Airy stress functions is equal to the number of states of self-stress.

Following the diagram in Figure 5 we start the algorithm by recognizing that there are no external loads applied to the structure. To be more specific there are no external loads applied to the structure that have a non-zero component parallel to the projection plane. Loads perpendicular to the projection plane do not show. When there are no external loads then all boundary nodes of Airy stress function are located on a single plane. One may see the Airy stress function extends at a horizontal zero plane to the infinity on all sides or often the Airy stress function is visualized as plane faced polyhedron with a flat bottom. Let's denote the edge nodes of the Airy stress function that are constrained to the horizontal zero plane with full black circles. Airy stress function for structures with horizontal thrust or reactions at the boundary would have ridges or valleys extending to infinity. These stress functions can be revised with an additional of virtual perimeter elements that resolve these thrust forces. By doing so the Airys stress function can be represented by a closed polyhedron, however, its bottom may contain multiple plane faces.

The second step of the procedure is to establish Airy stress values of preselected nodes that are necessary to obtain Airy stress values for all other nodes of the projected truss. These preselected nodes can be chosen all together at the beginning of the process or added one-by-one whenever necessary during the process of defining the plane faces of the Airy stress function. The preselected nodes are denoted with blue circles. The number of the preselected nodes needed to define full Airy stress function may differ depending on which nodes are preselected.

The third step is to recognize that 3 nodes in any planar face define Airy stress values for all nodes in this face. The diagram below indicates the order in which the rest of the nodes are calculated indicating groups of 3 nodes used to calculate "lifts" of other nodes in each plane. As we complete this step, we observe that a few nodes in the structure can be defined by combinations of different groups of 3 nodes. These instances, marked with yellow, we call conflicts.

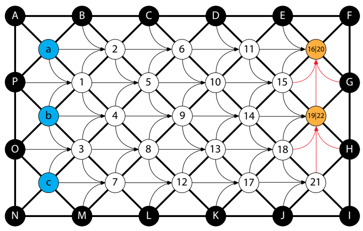

Figure 5: States of self-stress - graphical algorithm

Number of preselected blue nodes minus number of conflicts equals the number of states of self-stress that are unconditional and will always be present in the structure regardless of its topology. Number of remaining preselected nodes indicates number of candidates of additional conditional states of self-stress. These stresses may be possible under condition the nodes are placed in proper locations. The existence of conflict nodes does not indicate additional states of stresses can be obtained. In the example below we have 3 preselected blue nodes and 2 conflicts. Therefore, the projection of the grid-shell will always have at least one unconditional state of self-stress and possibly 2 other conditional states of self-stress. The grid-shell will not have more than 3 states of self-stress.

7. Counts

Vertical projection of each spanning grid-shell may be viewed as a mathematical graph. Understanding graph theory (Trudeau [3]), graphics statics (Zalewski, Allen [4], Wolfe [5], Cremona [6], Bow [7], Klein Wieghardt [8]), Airy stress function (Airy [9]) and force density form finding method (Schek [2]) helps navigate through the form finding of grid-shells, however these topics are too large to be discussed in this paper. What can be extracted from these mentioned theories are counts that may lead to interesting conclusions of studies structures.

First count would be for all plane-faced closed polyhedrons the following is true (Baker et. al. [10]):

$$v - b + f = 2 \tag{3}$$

where:

v − vertices or nodes

b − bars or edges

f − faces or polygons

Second is the Maxwell-Calladine [11] count:

$$2v - b - 3 = m - s \tag{4}$$

where:

m − number of linearly independent mechanisms

s − number of linearly independent states of self-stress

From (4) can be concluded that if a grid has no mechanisms, i.e., it is triangulated in a way that does not allow any mechanisms the count directly gives the number of states of self-stress. It is possible with preselection of number of nodes equal to the number of states of self-stress to define full Airy stress function.

Considering a reciprocal force diagram generated through theory of graphic statics the following is true (Baker et al [12]):

$$m + s = m^* + s^* \tag{5}$$

$$m - s = s^* - m^* - 2 \tag{6}$$

where * denotes the reciprocal diagram

In addition, there are other important counts discussed in Section 6 which are the count of preselected nodes and the count of conflict nodes. The number of preselected nodes equals the potential number of states of self-stress. In cases where the number of preselected nodes is larger than the number of conflict nodes the difference is the number of unconditional states of self-stress. Otherwise, the number of states of self-stress above one is not guaranteed.

8. Resolving conflicts and sensitivity of the incompatibilities of conflicts

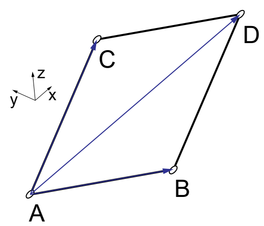

Figure 6: Planarity in 3D space

Starting from planarity constraint for a polygon in Figure 6, mixed product of 3 vectors is zero:

$$\overrightarrow{AD} \cdot \left(\overrightarrow{AC} \times \overrightarrow{AB}\right) = 0 \tag{7}$$

Where 3D locations of nodes A, B, C are known and z-coordinate of node D is to be calculated.

The following relation defines z-coordinates of a node D on an ABC plane:

$$D_z = A_z - \frac{\overrightarrow{AD}_x\left(\overrightarrow{AC}\times\overrightarrow{AB}\right)_x+\overrightarrow{AD}_y\left(\overrightarrow{AC}\times\overrightarrow{AB}\right)_y}{\left(\overrightarrow{AC}\times\overrightarrow{AB}\right)_z} \quad (8)$$

After differentiating we get:

$$\frac{\partial D_z}{\partial A_x} = \frac{\left(\left(\overrightarrow{AC}\times\overrightarrow{AB}\right)_x+\overrightarrow{AD}_y\overrightarrow{CB}_z\right)}{\left(\overrightarrow{AB}\times\overrightarrow{AC}\right)_z} - \frac{\left(AD_x\cdot\left(\overrightarrow{AC}\times\overrightarrow{AB}\right)_x+\overrightarrow{AD}_y\left(\overrightarrow{AC}\times\overrightarrow{AB}\right)_y\right)\cdot\overrightarrow{CB}_y}{\left(\overrightarrow{AB}\times\overrightarrow{AC}\right)_z^{\ 2}}, \quad (9)$$

$$\frac{\partial D_z}{\partial A_y} = \frac{\left(\left(\overrightarrow{AC}\times\overrightarrow{AB}\right)_y+\overrightarrow{AD}_x\overrightarrow{BC}_z\right)}{\left(\overrightarrow{AB}\times\overrightarrow{AC}\right)_z} - \frac{\left(AD_x\cdot\left(\overrightarrow{AC}\times\overrightarrow{AB}\right)_x+\overrightarrow{AD}_y\left(\overrightarrow{AC}\times\overrightarrow{AB}\right)_y\right)\cdot\overrightarrow{BC}_x}{\left(\overrightarrow{AB}\times\overrightarrow{AC}\right)_z^{\ 2}}, \quad (10)$$

and the following sensitivity equations:

$$\frac{\partial D_z}{\partial A_x} = \frac{\left(\overrightarrow{AB}\times\overrightarrow{AC}\right)_x+\left(\overrightarrow{AD}\times\overrightarrow{CB}\right)_x}{\left(\overrightarrow{AB}\times\overrightarrow{AC}\right)_z}, \quad (11)$$

$$\frac{\partial D_z}{\partial A_y} = \frac{\left(\overrightarrow{AB}\times\overrightarrow{AC}\right)_y+\left(\overrightarrow{BC}\times\overrightarrow{AD}\right)_y}{\left(\overrightarrow{AB}\times\overrightarrow{AC}\right)_z}, \quad (12)$$

$$\frac{\partial D_z}{\partial A_z} = 1 + \frac{\left(\overrightarrow{AD}\times\overrightarrow{CB}\right)_z}{\left(\overrightarrow{AB}\times\overrightarrow{AC}\right)_z}, \quad (13)$$

$$\frac{\partial D_z}{\partial D_x} = -D_x\frac{\left(\overrightarrow{AC}\times\overrightarrow{AB}\right)_x}{\left(\overrightarrow{AC}\times\overrightarrow{AB}\right)_z}, \quad (14)$$

$$\frac{\partial D_z}{\partial D_y} = -D_y\frac{\left(\overrightarrow{AC}\times\overrightarrow{AB}\right)_y}{\left(\overrightarrow{AC}\times\overrightarrow{AB}\right)_z}, \quad (15)$$

For each "conflict" node D_z can be calculated using more than one single group of three known nodes *A*, *B*, *C*. Number of linearly independent states of self-stress will equal to the number of preselected blue nodes that can each be lifted separately such that *z*-coordinates of all "conflict" nodes is the same regardless of which group of *A*, *B*, *C* nodes are used to calculate them. If the *z*-coordinates are not the same an adjustment of *xy* locations of nodes in the grid-shell may bring these values together. The direction the nodes should be relocated to minimize the incompatibility is informed by the sensitivity functions derived above and the dependency diagram like the one presented in Figure 5. Sensitivity of nodes belonging to disjoined polygons will require a chain rule calculation following an order of nodes that are reversed to the order of faces that have been used when calculating *z*-coordinates at the "conflict" nodes.

8. Examples

First, example will be a grid presented in Figure 5. The layout of the structure will be constrained to original double symmetry with constrained exterior nodes. Initial test, presented in Figure 7, shows that independent lifting of 3 preselected nodes is not possible without violating continuity of Airy stress function. Combination of lifts can maintain compatibility and represents a single state of self-stress possible for this geometry (Figure 7d).

After moving selected nodes along x direction, the incompatibilities are removed, and the three independent states of self-stress are shown in Figure 8.

Second example is based on the spider web diagram from the design of structural "spider webs" paper (Baker et al [10]) The count presented in the paper indicates the structure has at the most 3 states of self-stress (see 3 blue nodes that are preselected in Figure 9). The geometry of the original structure in the referenced paper has been obtained by freely placing the perimeter nodes and then assigning force density values to all members. By doing so the layout will always have at least one state of self-stress.

Can the net have more than one state of self-stress or can the geometry be updated in a way to have more than a single state of self-stress? How would geometry look like?

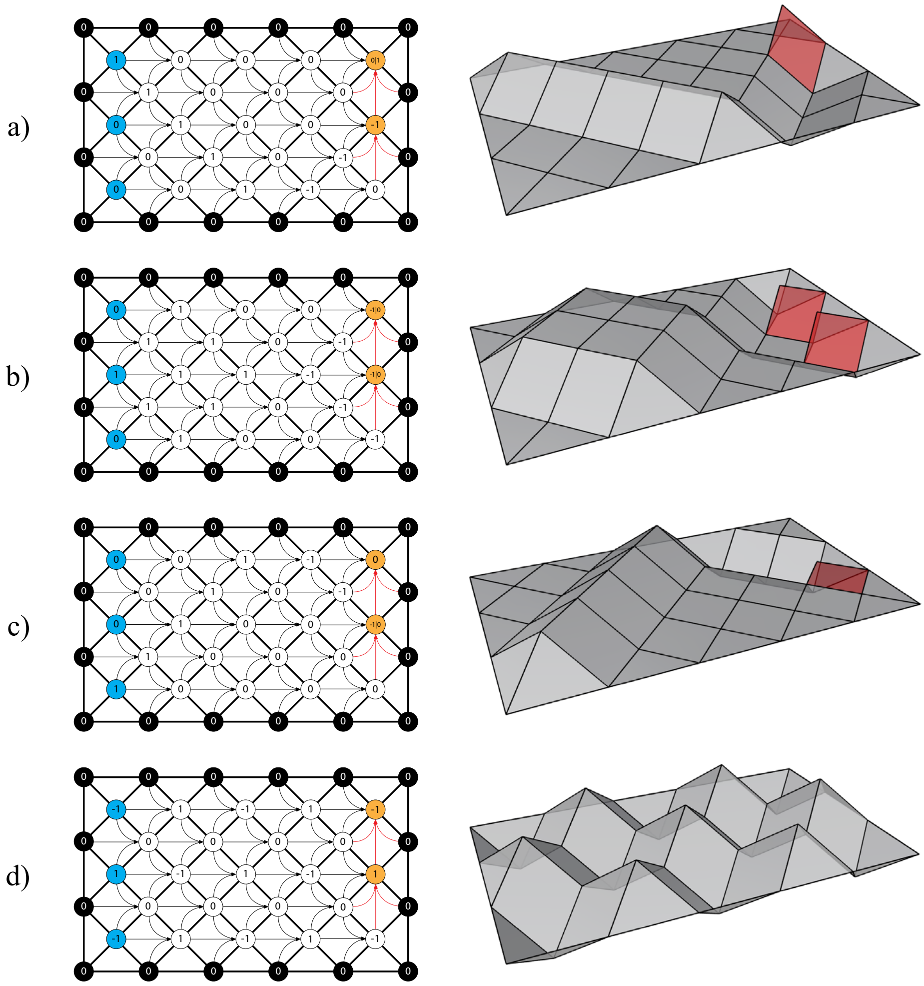

Figure 7: State of self-stress – initial check. a) through c) are incompatible states, d) is the single state of self-stress for the given geometry

To generate a similar structure in this paper the perimeter nodes are placed at the corners of a square, the force density of all internal elements except the center oculus is assigned to a value of $q = 1.0$. For oculus members $q \approx 7.4$ and perimeter members $q \approx 12.8$. Performing an initial test on the geometry we find that lifting one preselected node at the time does not generate closed plane faced polyhedron. These incompatible states of self-stress are not presented here. Figure 9 shows a single state of self-stress constructed using a non-zero lifts of the preselected nodes. The lift values are shown in the figure.

After following the states of self-stress maximizing algorithm a solution presented in Figure 10 is obtained. The obtained geometry can be funicular to 3 independent loads. Linearly independent states of self-stress for these loads are shown.

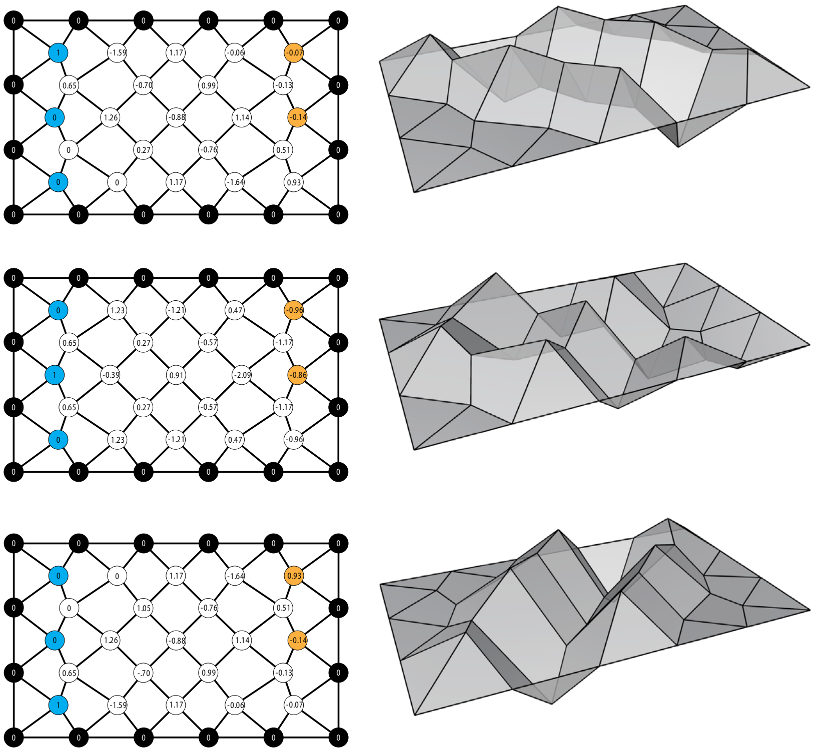

Figure 8: State of self-stress maximizing – final check

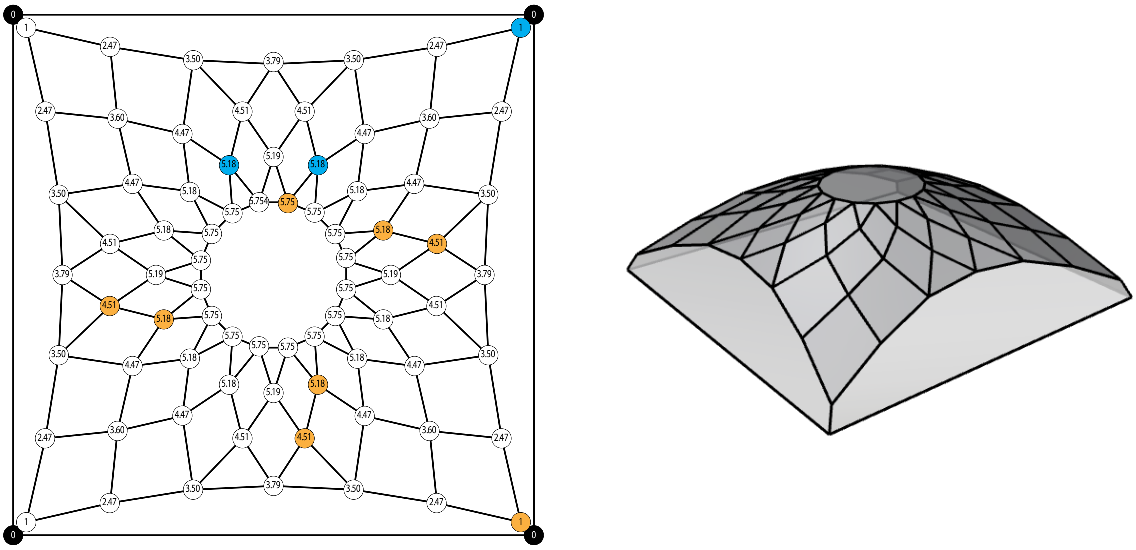

Figure 9: State of self-stress– the single state of self-stress for the given geometry

a)

b)

c)

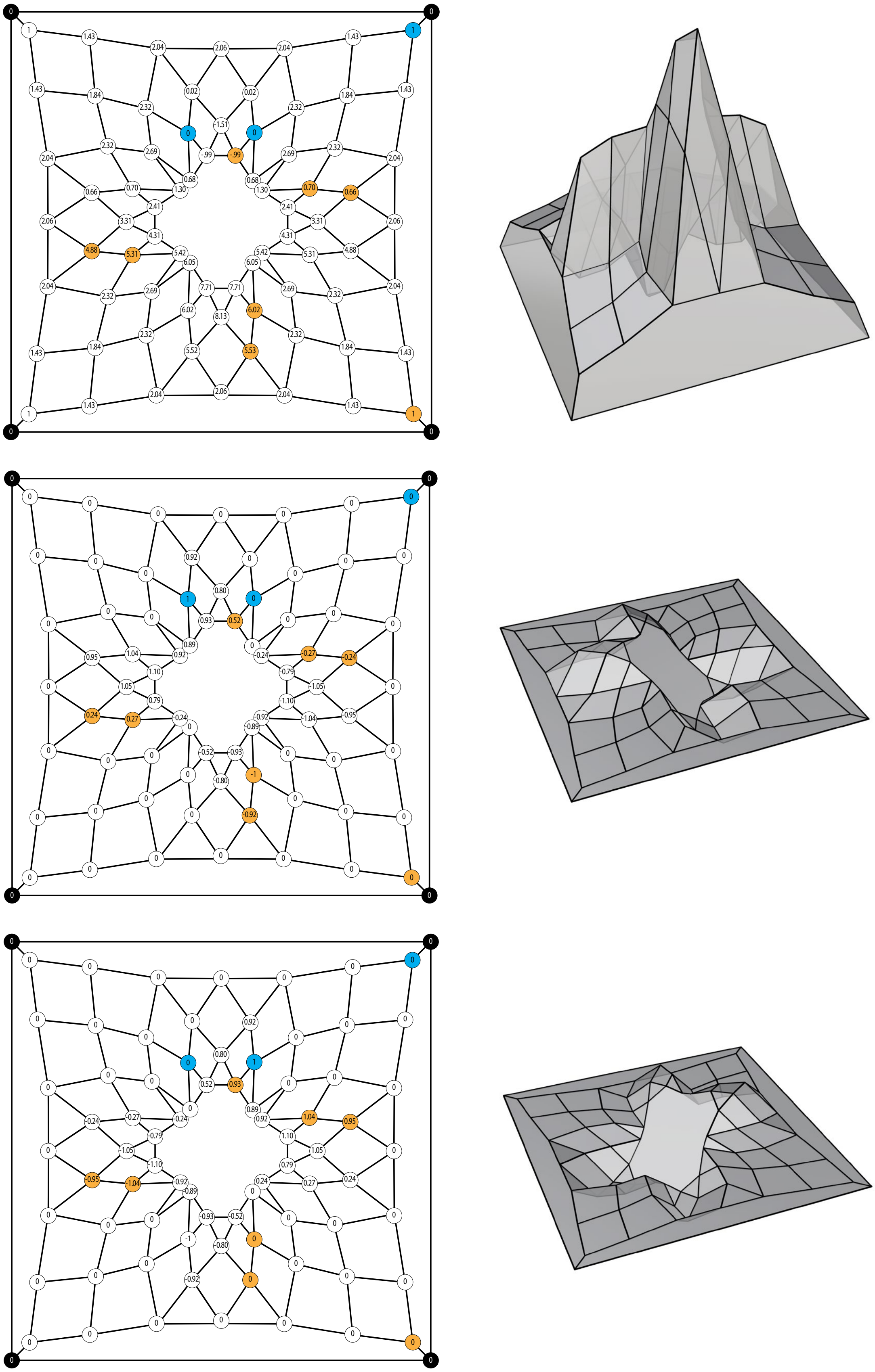

Figure 10: States of self-stress– linearly independent three states of self-stress after revising locations of nodes. Shapes of the Airy stress functions will depend on the selection of lift points (blue nodes)

9. Conclusion: submission of contributions

It is unlikely that an arbitrary grid-shell has maximum number of states of self-stress. However, often only minor relocation of nodes leads to the remaining states being available. With every added state of self-stress, a grid-shell is funicular to an additional load. Often these additional states of self-stress reduce the maximum design bending moments generated by all the design loads. It must also be understood here, that added states of self-stress correspond to additional mechanisms. These mechanisms may produce destabilizing motions that have to be prevented by the designer via moment connections or additional bracing members.

References

[1] Maxwell J (1870) On Reciprocal Figures, Frames, and Diagrams of Forces, Edinburgh Royal Society Proceedings 7:160–208

[2] Schek H. J., 1974, The force density method for form finding and computation of general networks, Computer Methods in Applied Mechanics and Engineering, 3(1), 115–134.

[3] Richard J. Trudeau, 1994, Introduction to Graph Theory, Dover Publications

[4] Zalewski W, Allen E, 1998, Shaping structures: statics. Wiley, New York

[5] Wolfe, W.S., 1921, Graphical Analysis a Text Book in Graphic Statics, McGraw-Hill Book Company, Inc, New York

[6] Cremona L, 1872, Le figure reciproche nella statica grafica, Milano, Tipografia di G. Bernardoni,

[7] Bow R, 1873, Economics of construction in relation to framed structures, ICE Publishing, London

[8] Klein F, Wieghardt K, 1904, Über Spannungsflächen und reziproke Diagramme, mit besonderer Berücksichtigung der Maxwellschen Arbeiten, Archiv der Mathematik und Physik, 8(3), p1–10 and 95–119

[9] Airy G. B., 1863, IV On the strains in the Interior of beams, Philosophical Transactions of the Royal Society of London, 153, pp. 49-79

[10] Baker, W.F., Mazurek, A. and Hartz, C. (2018), The design of structural ”spider webs“. Steel Construction, 11: 118-124. https://doi.org/10.1002/stco.201810018

[11] Calladine, C. R. 1978, Buckminster Fuller's 'Tensegrity' structures and Clerk Maxwell's rules for the construction of stiff frames, Int. J. Solids Structures, 14, 161–172

[12] Baker W F, McRobie A, Mitchell T, Mazurek A, 2015, Mechanisms and states of self-stress of planar trusses using graphic statics, Part I: Introduction and background, Proceedings of the International Association for Shell and Spatial Structures (IASS), Symposium 2015, Amsterdam